Development of High Precision Test Masses for the MICROSCOPE Space Project

Daniel Hagedorn, Heinz Peter Heyne, Stephan Metschke, Uwe Langner, Vincent Lebat, Manuel Rodriguez, Pierre Touboul, Frank Löffler

Development of High Precision Test Masses for the MICROSCOPE Space Project

Daniel Hagedorn[1, a *], Heinz-Peter Heyne[1,b], Stephan Metschke[1,c], Uwe Langner[1,d], Vincent Lebat[2,e], Manuel Rodriguez[2,f], Pierre Touboul[3,g], and Frank Löffler[1,h]

[1]Physikalisch-Technische Bundesanstalt, Bundesallee 100, 38116, Germany

[2]Office National d'Etudes et de Recherches Aérospatiales (ONERA), 29 avenue de la Division Leclerc, 92320 Châtillon, France

[3]ONERA, Chemin de la Hunière, BP 80100, 91123 PALAISEAU CEDEX Palaiseau, France

[a]daniel.hagedorn@ptb.de, [b]heinz-peter.heyne@ptb.de, [c]stephan.metschke@ptb.de, [d]uwe.langner@ptb.de, [e]vincent.lebat@onera.fr, [f]manuel.rodriguez@onera.fr, [g]toboul@onera.fr, [h]frank.loeffler@ptb.de

* corresponding author

Keywords: Fundamental Physics, Traceable Precision in-situ Measurement, Machining of Ductile Material, Process development

Abstract

The MICROSCOPE (MicroSatellite à traînée Compensée pour l'Observation du Principe d'Equivalence) project is an orbit-based mission to verify the Weak Equivalent Principle with an uncertainty of 10^{-15}. To achieve this goal two differential accelerometers, each equipped with two high precision test masses (made of PtRh10 and TiAl6V4 in the form of hollow cylinders with four flats at the outer shell and six precision countersinks at each face), are to be launched in Spring 2016 and shall orbit the earth for approx. one and a half year.
This paper describes the fundamental challenges of the test-mass fabrication on the basis of the requirements of the overall space project and the means developed to integrate in-situ measurement equipment into the precision fabrication station to link the internal probes to traceable standards.

Nomenclature

WEP = Weak Equivalence Principle
MICROSCOPE = MicroSatellite à traînée Compensée pour l'Observation du Principe d'Equivalence
ONERA = Office national d'études et de recherches aérospatiales
CNES = Centre national d'études spatiales
PTB = Physikalisch-Technische Bundesanstalt
ZARM = Zentrum für angewandte Raumfahrttechnologie und Mikrogravitation

Introduction

The Weak Equivalence Principle (WEP), i.e. the assumption that acceleration is independent from mass or composition of a respective body and cannot be distinguished from gravity for free falling objects, was drafted by Galileo Galilei in the late 16th and early 17th century. The physically and mathematically elaborated WEP is the very foundation of Albert Einstein's theory of

gravitation, i.e. General Relativity. Today, theoretical developments [1] suggest a possible range of WEP violation [10^{-14} – 10^{-21}] as a consequence of the coupling between matter and the string dilaton. Testing the WEP with an uncertainty of 10^{-15} is therefore of major interest regarding the verification of alternative theories of gravitation.

To date, the best ground experiments have been conducted by the EötWash group [2] with an uncertainty of (0.3 +/-1.8) x 10^{-13} using Copper, Aluminum, Silica, Titanium and Beryllium test-masses on torsion pendulums. Besides statistical errors, the most significant sources of perturbations are time variations of gravity gradients and thermal noise. Disturbance of gravity gradients originate mainly from seismic and human activities, building stability, gravity gradients of nearby hills and motion of water in the atmosphere as well as in the lithosphere. The resolution might be improved by no more than one order of magnitude over the next five years.

The European MICROSCOPE mission is an orbital, fundamental physics experiment led by the French Space Agency, CNES. The experiment was proposed by the Observatoire de la Cote d'Azur and ONERA [3, 4], in the frame of the CNES Myriad micro-satellite program, s fig. 1. Performing the WEP test in space reduces all gravitational disturbances due to seismic noise or human activity below relevant limits. The remaining residual gravity disturbance caused by the satellite's thermal expansion has been estimated to be less than $2x10^{-16}$ ms^{-2} and is thus compatible with the mission objectives. Moreover, one can take advantage of long measurement periods during the 18 months mission duration providing about 1,200 useful orbits for the benefit of rejection of stochastic disturbances.

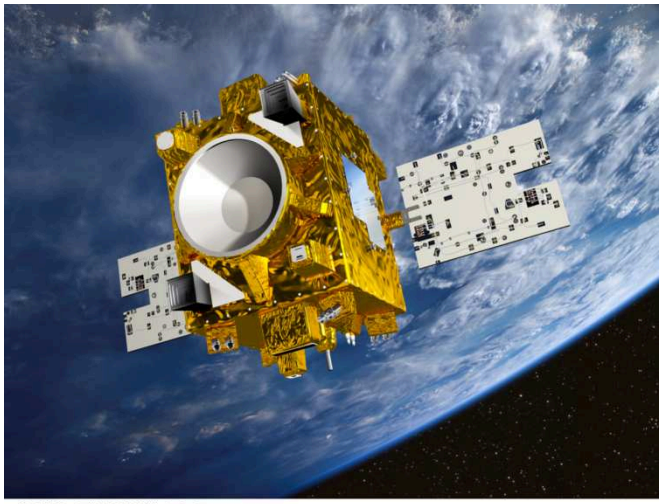

Fig. 1 Photo-composition of an Myriad mirco-satellite

At the core of the MICROSCOPE satellite, the payload is composed of two differential electrostatic space accelerometers, see illustration in Fig. 2. Each of the accelerometers contains one pair of test-masses, a combination of a PtRh10 inner and a TiAl6V4 outer test-mass for the first one and two PtRh10 test-masses for the second one. The electrodes, necessary to electro-statically control the test-masses, are made of gold coated silica. The silica parts are fabricated by a specific ultra-sonic machining process that allows an accuracy of a few micrometers when assisted by laser interferometry serving as in-situ fabrication control. The first instrument serves to test the WEP, while results from the second one shall help to eliminate systematic errors as no violation signal is obviously expected for the same test-mass material.

MICROSCOPE Space Experiment

Measurement Equations and Performance Objective

With regard to Galilei's basic considerations, an ideal test of the WEP would use two spherical test-masses exhibiting identical radii and consisting of a perfectly homogeneous density distribution located at the same point in space. Of course, such a configuration cannot be realized in practice, hence, test-masses in the form of hollow cylinders have been selected which exhibit the same value of the inertia matrix along the three main axes as spheres. As a matter of fact, differences of inertia values induce a deviance in the angular measurement output of the accelerometer which is not solely depending on angular acceleration. For technical reasons, as described below, additional form features are required.

The requirements concerning the accuracy of the test-mass geometry are deduced in the following. In a perfect free fall, the test-mass acceleration is expressed by Newton's Law:

$$m_{Ik}\overrightarrow{\Gamma_{App,k}} = m_{Gk}\vec{g}(O_k),$$

where m_{Ik} is the inertial mass of the body placed in O_{k} and $\overrightarrow{\Gamma_{App,k}}$ its acceleration. In a uniform gravity field, the force exerted on the mass is given by $m_{Gk}\vec{g}(O_k)$, $\vec{g}$ expressing the gravity field and m_{Gk} the gravitational mass of the body.

The WEP implies $m_{Ik} = m_{Gk}$ and $\overrightarrow{\Gamma_{App,k}} = \vec{g}(O_k)$.

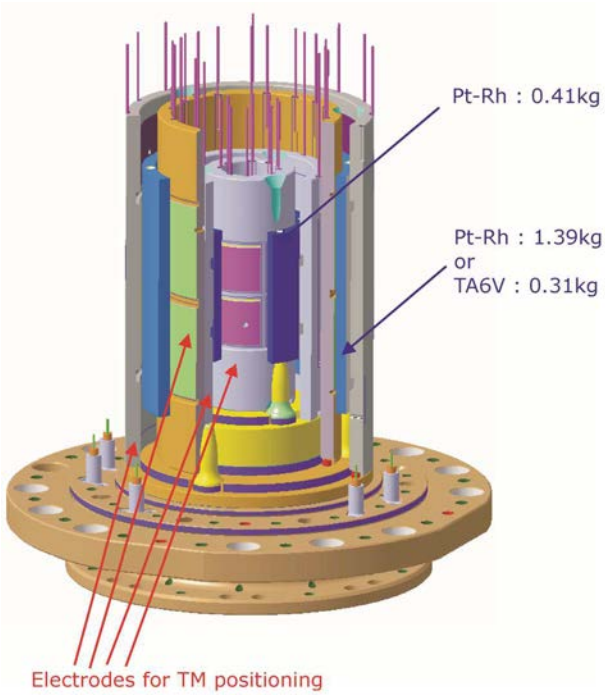

Fig. 2 Test-masses and the surrounding electrodes

The MICROSCOPE test-masses are motion-controlled using electro-static forces $\vec{F}el_k$ to maintain the bodies stationary with respect to the satellite which, in turn, is submitted to non-gravitational forces (drag, radiation pressure) $\vec{F}ext$ and to thruster actuations $\vec{F}th$. O_{sat} describes the

satellite's center of gravity. By finely measuring the difference of the electrostatic forces needed to maintain the two bodies in a motionless state, the equivalence of the acceleration of the two test-masses in one differential accelerometer can be deduced.

To take advantage of the accelerometer's performance, the satellite is maintained in an inertial pointing mode or slowly rotated about the axis normal to the orbital plane, s. Fig. 3. The Earth's gravity field is then projected either along the measurement axis at the orbital frequency or at the satellite rotation frequency in addition to the orbital frequency.

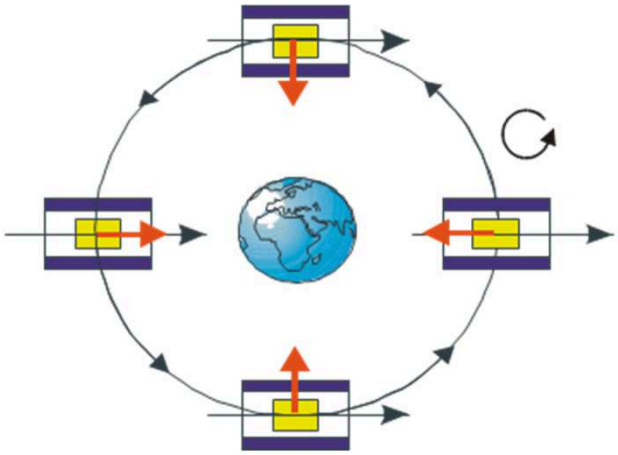

Fig. 3: Orbital motion of MICROSCOPE: measurement frame in black (always pointing to the right), gravitational field in red.

The acceleration applied to the mass k in the test-mass reference frame is expressed by:

$$\overrightarrow{\Gamma_{App,k}} = \frac{\vec{F}el_k}{m_{Ik}} =$$

$$\frac{M_{Gsat}}{M_{Isat}}\vec{g}(O_{sat}) - (1+\delta_k)\vec{g}(O_k) + R_{In,COR}\left(\overrightarrow{O_{sat}O_k}\right) - \frac{\vec{F}pa_k}{m_{Ik}} + \frac{\vec{F}ext}{M_{Isat}} + \frac{\vec{F}th}{M_{Isat}}$$

$$\frac{\vec{F}pa_k}{m_{Ik}}$$

expresses the contribution of the internal parasitic forces applied to each mass *k*, while

$$\frac{m_{Gk}}{m_{Ik}} = 1 + \delta_k$$

gives the ratio of the gravitational mass with respect to the inertial mass – which would differ from unity if the WEP is violated – and is depending on the test-mass material [1]. The gravitational mass MG_{sat} and the inertial mass MI_{sat} of the satellite are also considered.

$$R_{In,COR}\left(\overrightarrow{O_{sat}O_k}\right)$$

stands for the inertia and the Coriolis accelerations in the satellite frame due to the satellite attitude motion. If the test-mass electro-static control is sufficiently stiff, the residual relative motion can be neglected and the inertia effect is simply expressed by:

$$\dot{\vec{\Omega}} \wedge \overrightarrow{O_{sat}O_k} + \vec{\Omega} \wedge (\vec{\Omega} \wedge \overrightarrow{O_{sat}O_k})$$,

where $\vec{\Omega}$ represents the angular velocities of the satellite with respect to the inertial reference frame.

Finally, the differential acceleration applied on the two test-bodies (i) and (j) is given by:

$$\overrightarrow{\Gamma_{App,i}} - \overrightarrow{\Gamma_{App,j}} = (\delta_j - \delta_i)\vec{g}(O_j) + (1+\delta_i)[T]\overrightarrow{O_iO_j} -$$

$$R_{In,COR}\left(\overrightarrow{O_iO_j}\right) - \frac{\vec{F}pa_i}{m_{Ii}} + \frac{\vec{F}pa_j}{m_{Ij}}$$

$$= \overrightarrow{\Gamma_{app,i}} - \overrightarrow{\Gamma_{app,j}} - \frac{\vec{F}pa_i}{m_{Ii}} + \frac{\vec{F}pa_j}{m_{Ij}}$$

where O_iO_j is the distance between the two bodies and [T] is a linear approximation of the gravity field variations:

$$\vec{g}(O_j) - \vec{g}(O_i) = [T]\overrightarrow{O_iO_j} + \mathrm{O}(T2)$$

The second order gravity development terms T2 are indeed very small, leading to an acceleration residual smaller than $2\text{x}10^{-17}$ ms^{-2}.

$(\delta_j - \delta_i)\vec{g}(O_j)$ represents the violation signal of the WEP if it should exist.

The microsatellite will orbit the Earth at an altitude of 700 km. Here, the Earth's gravity has a value of 7.96 ms^{-2}. In order to detect a potential WEP violation at 10^{-15}, it is necessary to measure a difference of acceleration as small as

$$(\delta_j - \delta_i)\vec{g}(O_j) = 7.96\text{x}10^{-15}\ ms^{-2}$$

at the WEP test frequency. This is the objective of accuracy of the differential accelerometer [4]: all sources of error are evaluated and their contributions to the overall accuracy are summarized in the next subsections.

Test-Mass Centering Requirements

$$(1+\delta_i)[T]\overrightarrow{O_iO_j} \approx [T]\overrightarrow{O_iO_j}$$

represents the influence of the Earth's gravity gradient, as the test-mass alignment, in practice, cannot be perfectly concentric. The components of [T] have amplitudes of less than $5\text{x}10^{-9}$ ms^{-2}/m at the measurement frequency (i.e the orbital frequency with an inertial pointing satellite). As a result, the test-mass centering accuracy must be specified to 0.1 μm along the two directions of the orbital plane which are affected by the Earth's monopole term. However, this requirement cannot be met by any technology available.

Fortunately, the Earth's gravity is very well known, an achievement of the earlier space missions GRACE and GOCE [5]. By evaluating the effect of the Earth's gravity gradient at twice the orbital frequency, the off-centering is calibrated in the orbital plane and its effect at orbital frequency can be subtracted.

The application of this in-orbit procedure [4] allows to relax the requirement of the test-mass centering during integration to 20 µm. This specification must include the following error contributors:

- the electrostatic biasing,
- the machining limitations,
- the accuracy of the mounting process (integration).

The first one is due to electronics offsets of the position sensor which are falsely interpreted by the servo-loop accelerometer as a test-mass displacement. This contribution can be easily measured on ground while characterizing the electronics and has been optimized with respect to value and stability. Its overall contribution is less than 0.2 µm.

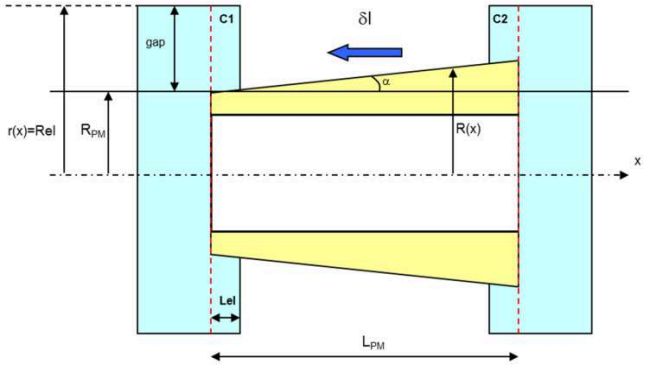

Fig. 4: Schema of a TM conicity for the capacitance sensing position of the test-mass TM along *X*

The second contributor to the off-centering is caused by deviations from the optimal geometry of the sensor core that modifies the electro-static field between the sensor electrodes and the test-masses. As shown in fig. 4, the operation of the electro-static loop will move the mass according to the defects of geometrical symmetry. When the test-mass moves towards the right, the capacitance on the right side, C2, increases while the capacitance on the left side, C1, decreases. Ideally, C1 equals C2, when the test-mass is centered. The electrostatic servo-loop acts to equalize the two capacitances and thus the test-mass remains steady and centered in the electrode frame (along X in this simple example). If the test-mass is cone-shaped (angle α), the servo loop will again displace the test-mass in order to equalize both capacitances. But, due to the small slope, C1 and C2 are not symmetric and the test-mass is displaced by δl evaluated in this case to:

$$C1 = C2 \text{ when } x = \delta l = -\alpha \frac{(L_{PM} - Lel)Lel}{2gap}$$

For one qualification test-mass model, the angle was $\alpha \approx 0.00067°$ (with translates into a deviation of about 7 µm over the whole length of 60.8 mm) leading to a generated miss-centering of 30 µm. To cope with this too large value, the electrode cylinder's form deviation could compensate the test-mass divergence. For the flight models, the machining procedures have been optimized and this defect has been reduced by one order of magnitude.

At last, the relative centering of the two concentric test-masses relies also on the mounting procedure of the overall accelerometer core. Accurate machining and permanent metrology enable to guarantee an accuracy of a few microns.

Acceleration Disturbances

Stochastic accelerations and systematic tone errors at the WEP measurement frequency must be considered. The difference of the parasitic acceleration applied on the two test-masses are represented by:

$$-\frac{\vec{F}pa_i}{m_{Ii}}+\frac{\vec{F}pa_j}{m_{Ij}}$$

Because of the use of a drag free configuration, the orbital motion can be maintained very stable. One can take advantage of very long, continuous integration periods offering a reduction of stochastic noise to a level of a few 10^{-15} ms^{-2}. The instrument's major source of noise, the mechanical residual damping of the test-mass, is of the order of $2x10^{-12}$ ms^{-2} $Hz^{-1/2}$. Integrating over 120 orbits (~$7x10^5$ s) reduces this contribution to $2.4x10^{-15}$ ms^{-2} at the WEP measurement frequency.

$$R_{In,COR}\left(\overrightarrow{O_{sat}O_k}\right)$$

represents the effect of the satellite's angular velocity or angular acceleration. This term can only be controlled by the satellite attitude system [4]. The values of acceleration along the 6 degrees of freedom are provided by the instrument itself and the satellite pointing system nullifies the angular acceleration measured by the 6 axis accelerometers.

Nevertheless, the angular and linear axes of the measurement are depending on the test-mass shape and inertia. Thus, the requirements of the test-mass geometry are deduced.

Test-Mass Development

Test-Mass Description

Each MICROSCOPE test-mass at the core of the differential accelerometers has the form of a hollow cylinder with four flat areas at the outer shell and six precision countersinks evenly distributed at each face. The flat areas as well as the faces are used to control the test-mass position, while the countersinks serve as seats for the blocking mechanism which clamps the test-masses during launch and limits the movement during operation.

The outer, larger test-masses of the differential accelerometers are made of either PtRh10 or TiAl6V4 test-masses. They exhibit an outer diameter of 69.395 mm, an inner diameter of 60.800 mm, and are 79.830 mm of length. The tolerances are 3 µm and below. The measures of the inner, smaller PtRh10 test-masses are: 34.400 mm (outer diameter), 30.800 mm (inner diameter), 43.332 mm (length). The same, strict tolerances of 3 µm and below apply.

TiAl6V4 is used in aeronautics and motor sports due to its low weight, combined with an excellent machinability and form stability below the range of 10 µm. Nevertheless, to achieve and maintain form and dimension stability below 5 µm, a multistage heat treatment and precisely adapted, low force turning and in-process lubrication and cooling parameters have to be applied.

PtRh10 on the other hand is a soft and ductile material and because of that not ideal for turning. However, due to the overall geometrical complexity of the test-masses with stringent requirements on shape, sizes and center of gravity, and because of the fact that each surface is referenced to all adjourning and opposite surfaces, turning is the technology of choice for the manufacturing of all test-masses [6].

Though it may seem that other methods of mechanical engineering like polishing or even electrical discharge machining (EDM) might be advantageous over turning, this is only true for single aspects of the overall fabrication work flow. Polishing, for example, would result in an improved surface roughness, especially of the PtRh10 alloy. Still, other parameters like concentricity or precision of (countersink) angles with their very low tolerances could not be achieved. Not at least the position and depth of the countersinks, especially on the second face, call for an exact knowledge of both, the test-mass and the tool positions. On a precision fabrication station, the whole manufacturing of the test-mass can be achieved in just two clamping positions, hereby minimizing the risk of damaging the delicate surfaces.

In-situ Measurements

In order to achieve the best possible results, it was found necessary to integrate high-precision measuring equipment into the fabrication station BENZINGER *TNI* for reasons described below.

As any form of mechanical machining is subject to tool wear, in most standard applications a mean time before tool wear-out or failure is determined, by which the tool has to be replaced. Among others, polycrystalline diamonds (PCD) cutting tools were investigated and produced the best results concerning both, tool-life and surface quality. During the development of the fabrication process for the MICROSCOPE test-masses it became obvious that this approach would not be applicable, because even small defects or extraordinary wear of the cutting tools due to surface anomalies may lead to a significant form deviation or even damage to the test-mass surface beyond repair. This is, of course, especially valid at the very end of the fabrication, when all dimension, form and surface roughness parameters have to be achieved in one finalizing cut.

It is important to recognize, though, that the fabrication tools use the same frame as the measuring equipment. It is because of this reason that two distinct adjustment steps are necessary.

Firstly, certified ring or plug gauges with the exact inner and outer diameters of the finished test-masses are mounted at the fabrication station's main axis, i.e. the fabrication axis. The gauge diameters are determined by contact measurement using a Renishaw OMP 400 high accuracy touch probe and passivated SiN balls to minimize adhesion. Several tens of points along the respective diameter are probed and from these data the best fitting circle and its respective diameter are calculated. The in-situ measurement verification of the inner and outer diameter has to pass a rigorous regime of measurement and repetition measurement. Only, if the comparison of all measurements shows a deviation of less than one micrometer, the adjustment is regarded successful.

Secondly, using a specially fabricated verification body, along several z-axis positions (z-axis being the central direction of the main fabrication axis) the inner and outer diameters are measured. Additionally, the distance from the verification body's center, the flatness and the angle of all four flats are measured, too. Hereafter, the verification body is being transferred to a coordinate measuring machine (CMM) and measured against calibrated gauges at the exact same positions. The results are in turn used to adjust the precision fabrication machine. The overall uncertainty budget has been verified to be less than two micrometers. Results above this limit are rejected and the procedures are repeated in total. By this approach, the measurements are traceable to the SI unit of length. Only the combination of both adjustment procedures guarantees reproducible results as defects of the frame itself cannot be detected using the first method only.

As a first fabrication step a thread is cut at one end of the hollow cylinder and the raw-mass is screwed against the dead stop of a custom made brass adapter. By this way the mounting forces are directed almost completely in z-direction and any relief of stress after unmounting the finished test-mass is reduced to the technical minimum, see Fig. 5.

Fig. 5: PtRh10 test-mass mounted at a brass adapter and testing probe inside the precision fabrication station

In this first clamping the first face, the inner and outer diameter, the four flats at the outer shell, the 45° angle chamfers connecting the faces and the inner and outer shell and the six countersink are fabricated. Form and aperture of the countersinks are determined by carefully selecting optimal styli, test drilling countersinks using identical materials and drilling parameters, measuring the test countersinks on a specialized CMM (ZEISS F25), and, additionally, allowing for tool wear.

Hereafter, the test-mass is unmounted and the thread is removed by means of wire EDM. Then the test-mass is mounted at the precision fabrication station again, this time using an adapted clamping system (Hainbuch company), which allows a secure clamping while, at the same time, not damaging the inner shell's surface.

Again, the motion control system of the precision fabrication station is being adjusted against a calibrated gauge block and then length, second face, and the final six countersinks are fabricated.

High-Precision ex-situ Measurements

After fabrication, the test-masses undergo extensive measurements. Besides form and dimension measurements [7], density, coefficient of thermal expansion (CTE), and mass of the test-masses are determined, also.

Form and dimension measurement consist of tactile measurements performed using a calibrated Leitz *reference* 600 CMM, see Fig. 6.

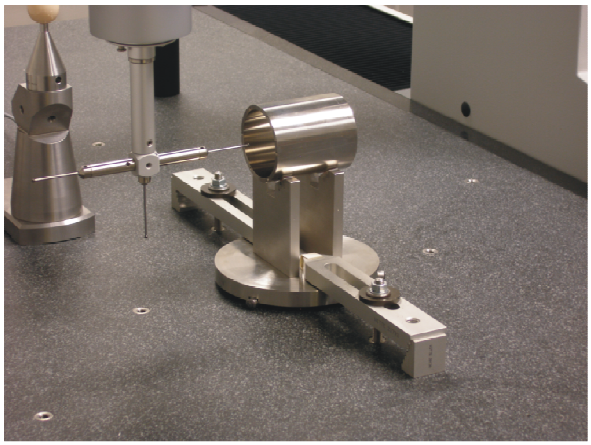

Fig. 6: One large Ti test-mass fixed at the measuring stand at the Leitz *reference* 600 CMM

Basically, for reasons of comparability, measurements are performed at the exact same positions as during fabrication, but with both, a higher resolution and at significantly more positions along the z-axis as well as close to both faces. From these results, all necessary features (diameters, length, concentricity, parallelism, planarity of both, the flats and the faces, position of countersinks) are determined. Fig. 7 shows a photo composition of the inner and the outer test-mass.

Tactile measurement has been chosen, since the accuracy of optical methods was found to be inadequate as a result of the roughness of the test-mass surfaces. While for the Ti alloy a surface roughness Ra ≈ 100 nm was achieved, which would allow the use of optical methods, the surface roughness of the PtRh10 was found to be about a factor of three higher, leading to a significantly larger error budget, when optical measurements were conducted during the development of the fabrication and measuring procedure.

As a rule, before and after the measurement of the test-masses, custom made calibrated gauges with diameters identical to those of the test-masses are being measured.

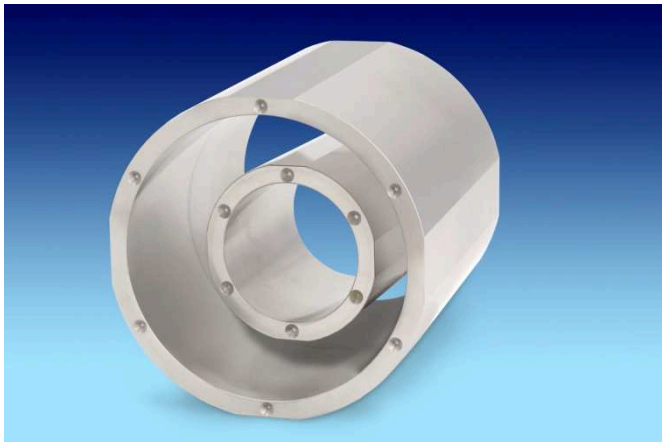

Fig. 7: Photo composition of both, inner and outer TM

Each test-mass is measured in four positions: horizontally mounted, inverse horizontally mounted, vertically mounted, and inverse vertically mounted. All measurement results have to comply with the two micrometer criterion of the overall uncertainty budget.

The countersinks are being measured using the ultra precision CMM ZEISS F25. Here, position, depth, aperture, and the angle of the countersink's central axis with respect to the faces are determined.

All additional measurements (density, coefficient of thermal expansion, and mass) are performed by PTB's dedicated laboratories.

The density of the test-masses is determined by direct measurement of all test-masses, but the large PtRh10 mass, because it is too heavy for the setup available. A density of app. 4.4 g/cm^3 for TiAl6V4 and 20 g/cm^3 for PtRh10 was measured. An uncertainty of up to 5x10^{-5} was reached.

The coefficient of thermal expansion is measured in the range from 18° C to 24° C with an uncertainty of 10^{-8}. As the space experiment is conducted at about 300 K, this is the range of choice. A CTE of 8.9 10^{-6} / K^{-1} (TiAl6V4) and 9.0 10^{-6} / K^{-1} (PtRh10) was determined.

Finally, the mass is measured with a precision of below 10^{-7}. Results: (large) TiAl6V4: approx. 300 g, small PtRh10: approx. 400 g, large PtRh10: approx. 1350 g.

Conclusions and Outlook

The MICROSCOPE space test of the Weak Equivalence Principle will be launched in 2016 on board a drag-free satellite. The experiment will be conducted on a polar orbit for about 18 month. The two differential accelerometers at the core of the experiment hold two test-masses each, comprising PtRh10 and TiAl6V4 alloys.

The 10^{-15} accuracy of the test, the electrostatic operation of the instrument, the capacitive position sensing of the test-masses, as well as the corrections of the test-mass off-centering require a demanding geometry of the test-masses. Extensive research has been carried out to develop the means for both, fabrication and measurement of the necessary core components, foremost the silica casing and the test-masses. A fabrication precision has been achieved, formerly unreached for these kinds of materials guaranteeing the necessary in-orbit centering accuracy of 20 µm. The flight

models of the test-masses were produced according to the established precisions and meet the mission requirements.

Though the experiment is not completed at the time of writing, the community is already discussing a follow-up mission. Several concepts are on the table, not the least of all the development of an orbit-based, superconducting accelerometer, which could improve the experiment's uncertainty down to the 10^{-18} range, but with even more stringent requirements on the test-masses.

Acknowledgement

PTB's Scientific Instrumentation Department would like to thank the dedicated PTB Departments of Mass (1.1), Analytics and Thermodynamic State Behaviour of Gases (3.2), Dimensional Nanometrology (5.2), Coordinate Metrology (5.3), and Interferometry on Material Measures (5.4) for their valuable support in metrological characterization of the test-masses.

The authors also want to acknowledge the CNES for their support and funding to develop the payload, the national aeronautics and space research center of the Federal Republic of Germany (DLR) for the support of the test-mass material, the Bremen ZARM center for their contribution to the qualification and acceptance tests of the payload in free fall conditions. Part of the work is funded by ONERA and PTB.

References

[1] T. Damour, A.M. Polyakov, "The string dilation and a least coupling principle," Nuclear Physics B, Vol. 423 Is.2-3 (1994) pp. 532-558.

[2] S. Schlamminger, K.-Y. Choi, K.-Y. Wagner, K.-Y. Gundlach, and E. Adelberger, "Test of the Equivalence Principle Using a Rotating Torsion Balance," Phys. Rev. Lett. 100, (2008) 041101.

[3] P. Touboul, M. Rodrigues, G. Métris, B. Tatry, "MICROSCOPE, testing the equivalence principle in space," Comptes Rendus de l'Académie des sciences (2001) IV-tome 2-N°9.

[4] P. Touboul, G. Métris, V. Lebat, and A. Robert, "The MICROSCOPE experiment, ready for the in-orbit test of the equivalence principle," Classical and Quantum Gravity 29 (2012).

[5] P. Touboul, B. Foulon, M. Rodrigues, J.P. Marque, "In orbit nano-g measurements, lessons for future space missions Aerospace," Science and Technology 8 (2004) 431-441.

[6] Hagedorn, D., Heyne, H.-P., Reimann, H., Neugebauer, M., Grüner, S., Metschke, St., Löffler, F., "Fabrication and Measurement Development for Precise Test Masses for the MICROSCOPE Space Project," ISBN 13: 978-0-9553082-6-0 (2009) 29-32.

[7] Jusko, O., Gerwien, N., Hagedorn, D., Härtig, F., Heyne, H.-P., Langner, U., Löffler, F., Metschke, St., Neugebauer, M., Reimann, H., "Final Manufacturing and Measurement of Satellite Proof Masses for the MICROSCOPE Project," Proc. ISPEMI 2010, 6th International Symposium on Precision Engineering Measurements and Instrumentation, Hangzhou, China, 8.-11.8.2010.